논문 2009-46SD-3-2

# 다중위상래핑과 실수값 함수를 이용한 효율적인 광 워터마킹

## ( Efficient Optical Watermark Using Multiple Phase Wrapping and Real-Valued Functions )

조 규 보*, 서 동 환**, 이 승 희***, 홍 재 근****

( Kyu-Bo Cho, Dong-Hoan Seo, Seung-Hee Lee, and Jae-Keun Hong )

요 약

본 논문에서는 다중위상래핑과 실수값 함수를 이용하는 효율적인 광 워터마킹을 제안하였다. 원 영상 삽입 과정에서 숨겨야 될 두 원 영상을 제로 패딩 시켜서 입력 평면의 두 개의 사분면에 하나씩 위치시킨 후 푸리에 변환을 수행하고 다중위상래핑을 적용하여 무작위 정 실수 값을 가지는 패턴을 생성시킨 후 하나의 실수부를 취하여 복호화 키를, 두 패턴 모두의 허수부의 합을 취하여 은닉영상을 생성시킨다. 위에서 생성된 은닉영상을 인간 시각으로는 감지 할 수 없도록 감쇄화 시킨 후 커버 영상과 일차 선형 변환 시켜서 배포영상을 제작한다. 복호화 과정에서는 배포영상과 복호화 키가 곱해져서 광학적인 역 푸리에 변환을 수행하고 출력 평면에서 원점에 대하여 대칭인 원영상이 간단히 복원된다. 컴퓨터 모의 실험과 광실험을 통하여 제안된 워터마킹이 광학적인 시스템에 적용 가능함을 확인하였다.

Abstract

In this paper, an efficient optical watermark method using multiple phase wrapping and real-valued decoding key is proposed. In the embedding process, two zero-padded original images placed in two quadrants on input plane are multiplied with two statistically independent random phase patterns and are Fourier transformed, respectively. Two encoded images are obtained by taking the real-valued data from these Fourier transformed images. And then two phase-encoded patterns, used as a hidden image and a decoding key, are generated by the use of multiple phase wrapping from each of the encoded images. A transmitted image is made from the linear superposition of the weighted hidden imagesand a cover image. In reconstruction process, the mirror reconstructed images can be obtained at all quadrants by the inverse-Fourier transform of the product of the transmitted image and the decoding key. Computer simulation and optical experiment are demonstrated in orderto confirm the proposed method.

**Keywords :** optical image watermarking, multiple phase wrapping, real-valued function

## I. Introduction

With the recent rapid growth of the technologies in computers, image-processing, optical devices, and internet, unlimited number of reproductions of the original contents can be created from unprotected digital contents. As a result, data hiding methods[1-2] have recently become important in many application areas as a method for preventing digital contents from illegal actions such as interception, duplication, and unauthorized distribution. These methods include the law of protection of intellectual property rights andan indication of content manipulation.

Data hiding methods should be capable of embedding an information, referred to as the hidden data, in another information, called the cover data and producing the transmitted data. The hidden data are

* 정회원, **** 평생회원, 경북대학교 전자전기컴퓨터학부
(School of Electronical Engineering & Computer Science, Kyungpook Nat'l Univ.)
** 정회원, 한국해양대학교 전기전자공학부
(Division of Electrical and Electronics Engineering, Korea Maritime Univ., Corresponding Author)
*** 정회원, 대경대학 e스포츠게임과
(Department of Esports Game, TaeKyeung Univ.)
접수일자: 2008년7월7일, 수정완료일: 2009년2월26일

used to place an indication of ownership in the cover data, answering the same purpose as an author's signature or a company logo, etc. The embedded or hidden data will be used hidden, unperceived, and invisible mean that an observer does not notice the presence of the data, even if unauthorized users are perceptible. The goal of data hiding is not to restrict or regulate access to the cover data, but rather to ensure that the embedded data remain inviolate and recoverable. Since the embedded data may face intentional and intelligent attempts to destroy or remove it, the coding method used must be immune to a wide variety of possible modifications, even if only a broken part of the transmitted data is available.

. Recently, many of image hiding methods using optics use the random noise to generate a random phase function that leads to be encoded onto other images and acts as security verification:[3~7] a random-phase computer -generated hologram (CGH),[3~4] off-axis hologram,[5~6] and modified joint transform correlator (JTC)[7] due to their high speed and parallel data processing. An approach that uses a random-phase CGH is suitable for pattern decomposition of a signature image. But the reconstruction algorithm which uses only inverse-Fourier transform is likely to be vulnerable to unauthorized use because of the absence of a decoding key and needs the computation time. Another approach that uses an off-axis hologram has been proposed and this method resists geometrical transformations, but it is not based on the real-valued system. So, above mentioned system is not applicable for the transmission system based on the real-valued system. A more robust approach using a modified JTC to decipher hidden data based on spatial correlation between two concealogram have been described; nevertheless, it still requires precise alignment and pixel-to-pixel mapping problems in the reconstruction process as it uses a 4-f correlator. In most of the previous methods based on optics, one of the merits is that they allow a complex representation of information. Therefore, the embedding and reconstruction of a complex image are easily performed and a high-quality reconstruction image can be obtained. However, in practical systems including electronic interfaces, for the image hiding method to be applied for practical transmission such as Internet transmission, a complex image must be replaced by real-valued patterns. Also, for practical transmission of transmitted images via the Internet, these images should be intensity maps with non-negative values in the previously proposed image hiding methods.

Accordingly, an efficient optical watermark method using multiple phase wrapping[8] and real-valued decoding key is proposed. The advantages of the proposed system are that phase wrapping is used to enhance the degree of security because the hidden image and the decoding key are randomly distributed and the transmitted image is not used in the reconstruction process and that a non-negative real-valued hidden image is used to solve the practical transmission of transmitted image via Internet. And pixel-to-pixel mapping and optical alignment problem are able to be solved because of serial connection scheme in proposed optical system.

In the embedding process, two zero-padded original images placed in two quadrants on input plane are multiplied by two statistically independent random phase patterns and are Fourier transformed, respectively. Two encoded images are obtained by taking the real-valued data from their Fourier transformed images. And then two phase-encoded patterns are generated by using the multiple phase wrapping from two encoded images. This approach is suitable for generating random patterns used as hidden images and a decoding key because the multiple phase wrapping performs a nonlinear mapping of the arithmetic patterns. In order to obtain a non-negative value for practical transmission, the sum of two imaginary parts of two patterns and the real part of the one pattern, whose phase ranges are reduced by the same visibility control factor, are used as the hidden image and the decoding key, respectively. A transmitted image is made from the linear superposition of the weighted hidden images and a coverimage. In reconstruction process, the mirror reconstructed images can be obtained at all quadrants by the inverse-Fourier transform of the product of the transmitted image and the decoding key. The product between the transmitted image and the decoding key and its inverse-Fourier transform operation can be realized by a serial connection in optical setup. The advantages of proposed setup are as follows. Serial connection used to solve the optical alignment problem and the original image is reconstructed without any information of the original image or previous 4-f setup. Moreover, because of the output images appeared at all quadrants, the allocation of the reconstructed image is efficient. Computer simulation and optical experiment are demonstrated in order to confirm the proposed method about robustness against attacks such as cropping or JPEG-compression.

## Ⅱ. Proposed watermarking

### 2.1 Imbedding process

Let $o_{z1}(x,y)$, $o_{z2}(x,y)$, $\exp[jn_1(x,y)]$, and $\exp[jn_2(x,y)]$ denote two zero-padded original images which are placed in two quadrants of the input plane and two random phase images, respectively, where $n_1(x,y)$ and $n_2(x,y)$ are white sequences uniformly distributed in $[0, 2\pi]$. First, assuming the input images are uniformly distributed in the Fourier plane, we multiply these original images with the random phase images, respectively and then perform the Fourier transform given by

$$O_1(\xi,\eta) = \mathrm{FT}\{o_{z1}(x,y)\exp[jn_1(x,y)]\},$$
$$O_2(\xi,\eta) = \mathrm{FT}\{o_{z2}(x,y)\exp[jn_2(x,y)]\}. \qquad (1)$$

Since the original images are zero-padded and Fourier transformed, the original information can be obtained by Fourier-transforming only the real-part

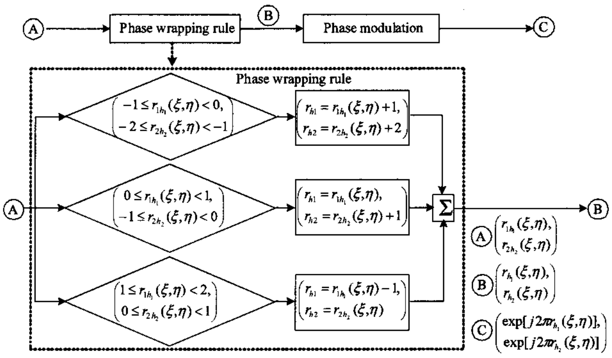


그림 1. 다중 위상 래핑을 이용한 은닉 영상 생성 블록도

Fig. 1. Block diagram for generating the hidden image using multiple phase wrapping.

of $O_1(\xi,\eta)$ and $O_2(\xi,\eta)$ called encoded images $E_1(\xi,\eta)$ and $E_2(\xi,\eta)$ which are normalized and distributed in [-1, 1], respectively. Here, the multiple phase wrapping[8] is applied to obtain two random phase-encoded patterns from the encoded image. Figure 1 shows the block diagram for generating the hidden image using multiple phase wrapping. Two arithmetic random phase-encoded patterns $\exp[j2\pi r_{1h}(\xi,\eta)]$ and $\exp[j2\pi r_{h_2}(\xi,\eta)]$ can be obtained by the arithmetic operation with two phase-encoded images given by

$$\exp[j2\pi r_{1h_1}(\xi,\eta)] = \exp[j2\pi\{E_1(\xi,\eta) + r_{d1}(\xi,\eta)\}],$$
$$\exp[j2\pi r_{2h_2}(\xi,\eta)] = \exp[j2\pi\{E_2(\xi,\eta) - r_{d2}(\xi,\eta)\}], \qquad (2)$$

where $r_{d1}(\xi,\eta)$ and $r_{d2}(\xi,\eta)$ used to generate the decoding key are randomly distributed in [0, 1]. The multiple phase wrapping performs a nonlinear mapping of the arithmetic random patterns $r_{1h_1}(\xi,\eta)$ and $r_{2h_2}(\xi,\eta)$ into $r_{h_1}(\xi,\eta)$ and $r_{h_2}(\xi,\eta)$ used to generate a hidden image given by

$$\exp[j2\pi r_{h_1}(\xi,\eta)] = \begin{cases} \exp\{j2\pi[r_{1h_1}(\xi,\eta)+1]\}, & -1 \le r_{1h_1}(\xi,\eta) < 0 \\ \exp\{j2\pi[r_{1h_1}(\xi,\eta)+0]\}, & 0 \le r_{1h_1}(\xi,\eta) < 1 \\ \exp\{j2\pi[r_{1h_1}(\xi,\eta)-1]\}, & 1 \le r_{1h_1}(\xi,\eta) \le 2, \end{cases}$$

$$\exp[j2\pi r_{h_2}(\xi,\eta)] = \begin{cases} \exp\{j2\pi[r_{2h_2}(\xi,\eta)+2]\}, & -2 \le r_{2h_2}(\xi,\eta) < -1 \\ \exp\{j2\pi[r_{2h_2}(\xi,\eta)+1]\}, & -1 \le r_{2h_2}(\xi,\eta) < 0 \\ \exp\{j2\pi[r_{2h_2}(\xi,\eta)+0]\}, & 0 \le r_{2h_2}(\xi,\eta) \le 1, \end{cases} \qquad (3)$$

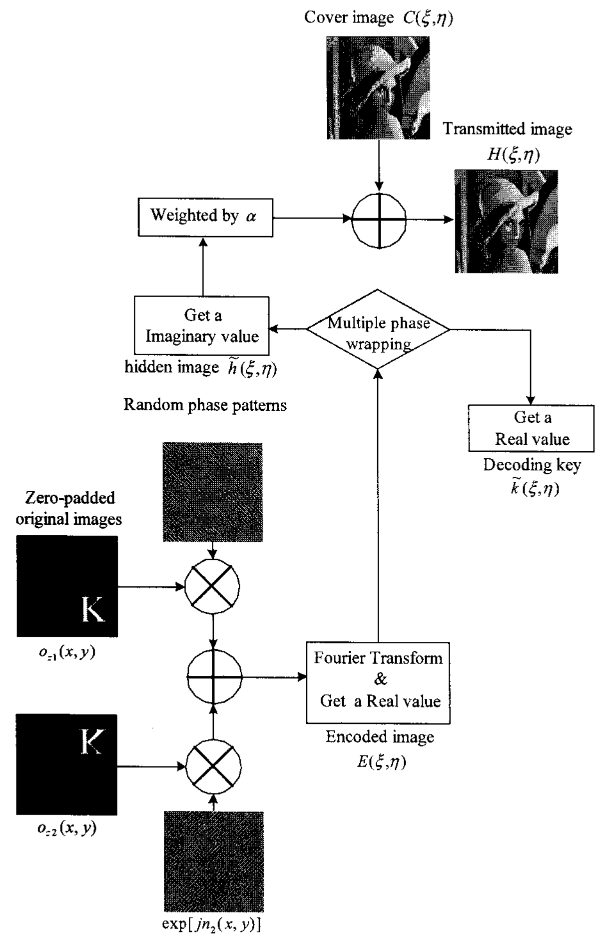


그림 2. 제안된 워터마킹 시스템의 영상 삽입 과정의 전체 블록도

Fig. 2. The perspective block diagram of the embedding process of the proposed watermarking system.

where $\exp[j2\pi r_{h_1}(\xi,\eta)]$ and $\exp[j2\pi r_{h_2}(\xi,\eta)]$ are phase wrapped using $\exp[j2\pi r_{1h_1}(\xi,\eta)]$ and $\exp[j2\pi r_{2h_2}(\xi,\eta)]$, which have the phase range $[0,2\pi]$. Each pixel value of the arithmetic random pattern is wrapped into the interval [0, 1] by the above rule. If the value of each pixel of $r_{1h_1}(\xi,\eta)$ is distributed in [-1, 0], [0, 1], and [1, 2], the value of $r_{h_1}(\xi,\eta)$ is wrapped into $r_{1h_1}(\xi,\eta)+1$, $r_{1h_1}(\xi,\eta)$, and $r_{1h_1}(\xi,\eta)-1$, respectively; and then $r_{h_1}(\xi,\eta)$ is phase-encoded into $\exp[j2\pi r_{h_1}(\xi,\eta)]$. And if the value of each pixel of $r_{2h_2}(\xi,\eta)$ is distributed in [-2, -1], [-1, 0], and [0, 1], the value of $r_{h_2}(\xi,\eta)$ is wrapped into $r_{2h_2}(\xi,\eta)+2$, $r_{2h_2}(\xi,\eta)+1$, and $r_{2h_2}(\xi,\eta)$, respectively; and then $r_{h_2}(\xi,\eta)$ is phase-encoded into $\exp[j2\pi r_{h_2}(\xi,\eta)]$ as in Fig. 1. Let $\tilde{h}(\xi,\eta)$ and $\tilde{k}(\xi,\eta)$ denote a hidden image and the decoding key given by

$$\begin{aligned}\tilde{h}(\xi,\eta) &= \mathrm{Im}\{\exp[j2\pi r_{h_1}(\xi,\eta)/K]+\exp[j2\pi r_{h_2}(\xi,\eta)/K]\}\\ &= \sin[2\pi r_{h_1}(\xi,\eta)/K]+\sin[2\pi r_{h_2}(\xi,\eta)/K],\end{aligned} \tag{4}$$

$$\tilde{k}(\xi,\eta) = \mathrm{Re}\{\exp[j2\pi r_{h_2}(\xi,\eta)/K]\} = \cos[2\pi r_{h_2}(\xi,\eta)/K],$$

where $\mathrm{Im}\{\cdot\}$, $\mathrm{Re}\{\cdot\}$, and integer $K$ denote the imaginary part of $\{\cdot\}$, the real part of $\{\cdot\}$, and the visibility control factor that controls the visibility of the reconstructed image by reducing the phase ranges of $\tilde{h}(\xi,\eta)$ and $\tilde{k}(\xi,\eta)$ in the reconstruction process, respectively. The notation of the variable is the same as the method using one original image. The transmitted image is then given by

$$H(\xi,\eta) = \alpha\tilde{h}(\xi,\eta) + C(\xi,\eta), \tag{5}$$

where $C(\xi,\eta)$, $H(\xi,\eta)$, and $\alpha$ denote the cover image which is distributed in [0, 1], the transmitted

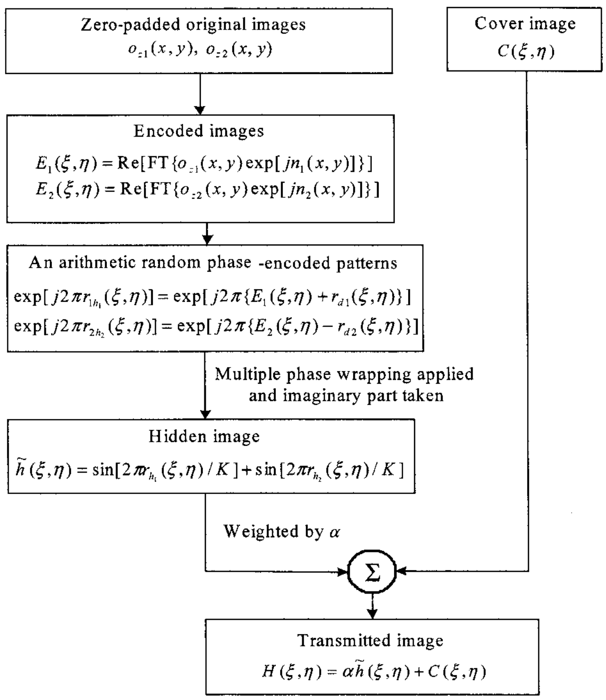


그림 3. 다중 위상 래핑을 이용한 제안된 워터마킹 시스템에 대한 삽입 과정의 세부 블록도

Fig. 3. The detailed block diagram of the embedding proces for the proposed watermarking system using the multiple phase wrapping.

image which is the linear superposition of the weighted hidden image and the cover image, and a coefficient chosen to control the invisibility of the hidden image. The notation of the variable is the same as the method using one original image. Figure 2 shows a perspective block diagram of the embedding system for the proposed watermarking method and the proposed detailed block diagram for the embedding system is shown in Fig. 3.

## 2.2 Reconstruction process

In order to reconstruct the original images, the transmitted image is directly multiplied by the decoding key and then is inverse-Fourier transformed.

The product between the decoding key and the transmitted image is given by

$$\begin{aligned}&\tilde{k}(\xi,\eta)H(\xi,\eta)\\&=\frac{\alpha}{2}\sin[2\pi\{r_{h_1}(\xi,\eta)-r_{d1}(\xi,\eta)\}/K]+C(\xi,\eta)\cos[2\pi r_d(\xi,\eta)/K]\\&+\frac{\alpha}{2}\sin[2\pi\{r_{h_2}(\xi,\eta)+r_{d2}(\xi,\eta)\}/K]+\text{other terms.}\end{aligned} \tag{6}$$

According to Eq. (6) and Taylor series expansion of trigonometric function, the first and the third term on the right-hand side of Eq.(6) can be expressed as

$$\begin{aligned}&\frac{\alpha}{2}\sin[2\pi\{r_{h_1}(\xi,\eta)-r_1(\xi,\eta)\}/K]\\&=\frac{\alpha}{2}\sin[2\pi E_1(\xi,\eta)/K]\approx\frac{\alpha\pi}{K}E_1(\xi,\eta),\quad\text{for } 2\pi E_1(\xi,\eta)<<K\\&\frac{\alpha}{2}\sin[2\pi\{r_{h_2}(\xi,\eta)-r_2(\xi,\eta)\}/K]\\&=\frac{\alpha}{2}\sin[2\pi E_2(\xi,\eta)/K]\approx\frac{\alpha\pi}{K}E_2(\xi,\eta).\quad\text{for } 2\pi E_2(\xi,\eta)<<K\end{aligned} \tag{7}$$

The value of $K$, for $2\pi E_1(\xi,\eta)<<K$ and $2\pi E_1(\xi,\eta)<<K$, plays the role of reducing the phase range in the third term in Eq. (6) and representing the approximation effect in Eq. (7). Then inverse-Fourier transform for Eq. (7) is obtained by

$$\begin{aligned}&\text{IFT}\{\tilde{k}(\xi,\eta)H(\xi,\eta)\}\\&=\text{IFT}\{\frac{\alpha\pi}{K}[E_1(\xi,\eta)+E_2(\xi,\eta)]\}+\text{other terms}\\&\approx e'(x,y)+r'(x,y).\end{aligned} \tag{8}$$

For simplicity, $e'(x,y)$ and $r'(x,y)$ are equal to $\text{IFT}\{\alpha\pi[E_1(\xi,\eta)+E_2(\xi,\eta)]/K\}$ and other terms, respectively. Then the reconstructed image $R_{\text{CCD}}(x,y)$ in the CCD plane is expressed as

$$\begin{aligned}R_{\text{CCD}}(x,y)&=|e'(x,y)+r'(x,y)|^2\\&=\left(\frac{\alpha\pi}{2K}\right)^2[o_{z1}'(x,y)]^2+\left(\frac{\alpha\pi}{2K}\right)^2[o_{z2}'(x,y)]^2\\&+\left(\frac{\alpha\pi}{2K}\right)[o_{z1}'(x,y)+o_{z2}'(x,y)]r'(x,y)^*\\&+\left(\frac{\alpha\pi}{2K}\right)[o_{z1}'(x,y)+o_{z2}'(x,y)]^*r'(x,y)+|r'(x,y)|^2\end{aligned} \tag{9}$$

where $\exp[jn'(x,y)]$ is the inverse-Fourier transform result for $\text{Re}[\text{FT}\{\exp[jn(x,y)]\}]$, and $o_{z1}'(x,y)$ and $o_{z2}'(x,y)$ denote a real and even reconstructed patterns which are the inverse-Fourier transform results for $\text{Re}[\text{FT}\{o_{z1}(x,y)\}]$ and $\text{Re}[\text{FT}\{o_{z2}(x,y)\}]$.

Also in Eq.(9), $\alpha\pi[o_{z1}'(x,y)+o_{z2}'(x,y)]r'(x,y)^*/2K$, $\alpha\pi[o_{z1}'(x,y)+o_{z2}'(x,y)]^*.\times r'(x,y)/2K$ and $|r'(x,y)|^2$ are pseudo-randomly dispersed like white noise with small value within the real and even reconstructed image and within the output plane, respectively. Therefore, the reconstructed images can appears to stand out over the dispersed noise image. Figure 4 shows the perspective block diagram of the reconstruction system for the proposed method and the proposed block diagram for the reconstruction system using decoding key are shown in Fig. 5.

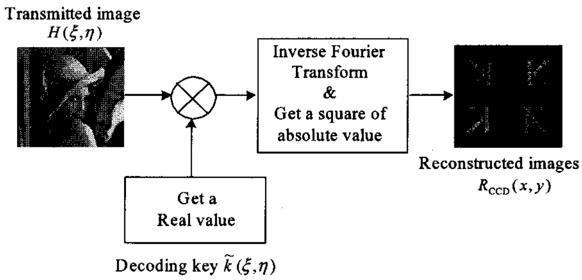


그림 4. 제안된 워터마킹 시스템의 복호화 과정의 전체 블록도

Fig. 4. The perspective block diagram for the reconstruction process of the proposed watermarking system.

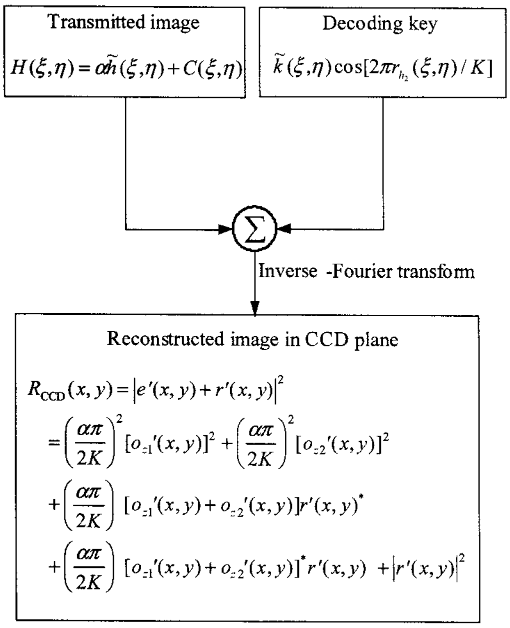


그림 5. 다중 위상 래핑을 이용한 제안된 워터마킹 시스템에 대한 삽입 과정의 세부 블록도

Fig. 5. The detailed block diagram of the proposed reconstruction process using the real-valued decoding key in case of the method with two original images.

## Ⅲ. computer simulations

We performed computer simulations to confirm the validity of the proposed method. As shown in Fig. 6(a), 6(b), $64\times 64$ pixel flipped "K" images are zero-padded to be $129\times 129$ pixel images and these zero-padded images are used in our computer simulation. Figures 6(c) and 6(d) are the encoded images which are the real-valued data of Fourier transform for the zero-padded original images and the reconstructed images which are positioned as mirror images, respectively.

Figure 7(a), 7(b), and 7(c) show the cover image, the hidden image generated from the encoded image, and the transmitted image, respectively. As same as one original image is used, the value $\alpha$ and $K$ are 0.02 and 20 in fig. 6 and 7, respectively. When the transmitted image and the decoding key are placed at matching positions in the reconstruction process, the decoding key with non-negative value and the corresponding recovered original image is shown in

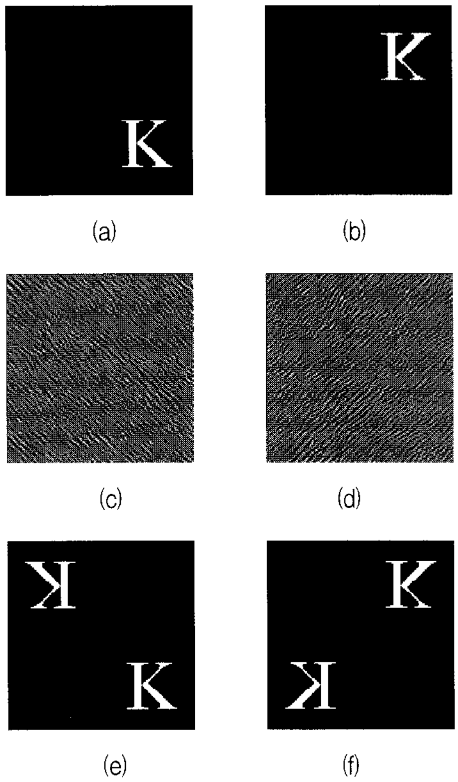


그림 6. 실수값 패턴에 의한 복호화: (a) 제 1 사분면에 위치한 제로 패딩 된 원영상 (영문자"K"), (b) 제 2 사분면에 위치한 제로 패딩 된 원영상 (플립된 영문자 "K"), (c) 그림 (a)에 관계 된 인코딩 영상, (d) 그림 (b)에 관계 된 인코딩 영상, (e) 그림 (a)의 복호화 영상, (f) 그림 (b)의 복호화 영상

Fig. 6. Reconstruction with real-valued patterns: (a) a zero-padded original image in the first quadrant (the letter "K"), (b) a zero-padded original image in the second quadrant (the reverse of the letter "K") (c) encoded image corresponding to (a), (d) encoded image corresponding to (b), (e) reconstructed image of (a), (f) reconstructed image of (b).

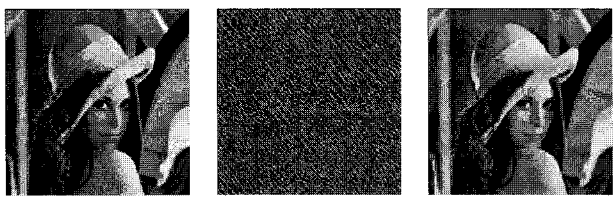

(a) (b) (c)

그림 7. 모의실험 상에서 삽입 과정에 사용 된 영상: (a) 커버 영상, (b) 은익 영상, (c) 전송 영상

Fig. 7. Images used in the embedding process in simulations: (a) cover image, (b) hidden image, (c) transmitted image.

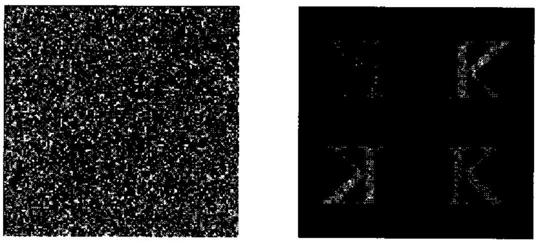

(a) (b)

그림 8. 모의실험 상에서 복호화 과정에서 사용된 영상: (a) 양의 값을 가진 디코딩 키 (b) 복호화 영상

Fig. 8. Images used in the reconstruction process in simulations: (a) decoding key with non-negative value, (b) reconstructed image.

Fig. 8(a) and 8(b), respectively. In Fig. 8(b), the background noise shown in Fig. 8(a) is due to residual component of the main lobe which is spatially block filtered and randomly dispersed noise of $|r'(x,y)|^2$. Here we use peak signal-to-noise ratio (PSNR) as a metric to evaluate the quality of the reconstructed images.[9] The PSNR between the two images $d(\xi,\eta)$ and $d_r(\xi,\eta)$ can be defined as

$$\text{PSNR} = 20\log_{10}\left\{\frac{2^n-1}{\sqrt{\frac{1}{M\times N}\sum_{\xi=0}^{M-1}\sum_{\eta=0}^{N-1}[|d(\xi,\eta)-d_r(\xi,\eta)|^2]}}\right\} \quad (10)$$

where $d_r(\xi,\eta)$ and $d(\xi,\eta)$ denote the input information and the reconstructed image, respectively. $M$ is the number of columns, $N$ is the number of rows, and $n$ is the number of bits representing a pixel. Figures 9 (a) and 9(b) show the values of PSNR are widely distributed. The increase of the PSNR should be nearly saturated at the value of $K$ which become about 200.

According to increasing the value of $\alpha$ and $K$, the value of PSNR increase and the performance seems to be enhanced. For a large value of $K$, background noise is decreased and due to reduction phase range of the hidden image, the transmitted image is almost unchanged by the hidden image. When the value of $\alpha$ increases, the transmitted image is distorted owing to increasing of the level of the hidden image. Hence the choice of $\alpha$ and $K$ depends on the relative

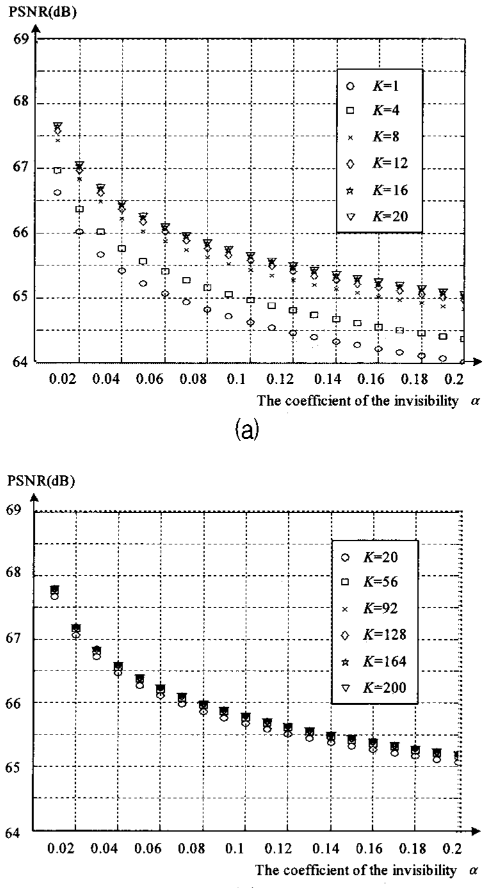


그림 9. $\alpha$값에 따른 원 영상과 복원 영상의 PSNR: (a) $K$값이 [0, 20]에 분포될 경우, (b) $K$값이 [20, 200]에 분포될 경우

Fig. 9. PSNR for both the original image and the reconstructed image based on the value of $\alpha$: (a) the case of the value of $K$ is distributed in [0, 20], (b) the case of the value of $K$ is distributed in [20, 200].

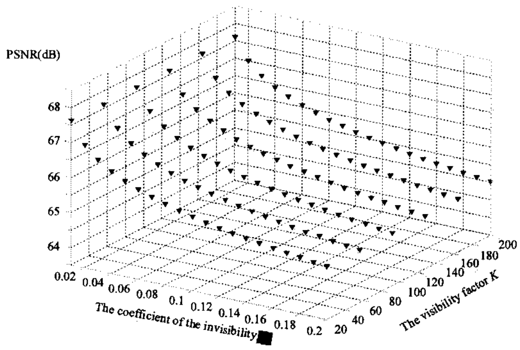


그림 10. $\alpha$와 $K$값에 따른 원 영상과 복원 영상의 PSNR

Fig. 10. PSNR for both the original image and the reconstructed image based on the value of $\alpha$ and $K$.

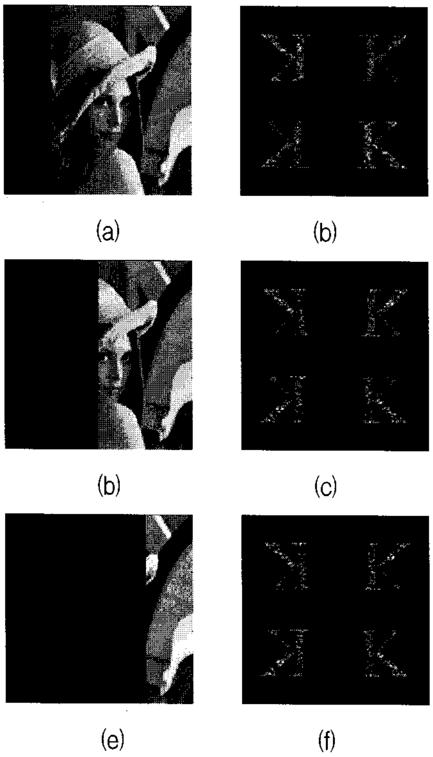


그림 11. 블록 된 전송 영상과 복원 영상: (a) 25% 블록 된 전송 영상, (b) 그림(a)에 관련 된 복원 영상, (c) 50% 블록 된 전송 영상, (d) 그림 (c)에 관련 된 복원 영상, (e) 75% 블록 된 전송 영상, (f) 그림 (e)에 관련 된 복원 영상

Fig. 11. Blocked transmitted images and reconstructed images: (a) 25% blocked transmitted image, (b) reconstructed image of (a), (c) 50% blocked transmitted image, (d) reconstructed image of (c), (e) 75% blocked transmitted image, (f) reconstructed image of (e).

importance of maintaining the appearance of the transmitted image unchanged and the visibility to reconstruct the original image. Figure 10shows the graph of PSNR for both the original image and the reconstructed image based on the value of $\alpha$ and $K$.

We check the robustness of this method when some pixels of the transmitted image are blocked by investigating the reconstructed image. Figures 11(a), 11(c), and 11(e) show that the transmitted images of 25%, 50%, and 75% are blocked along the $\xi$-axis, respectively.

When the transmitted image and the decoding key are placed at the matching positions in the reconstruction process, the corresponding recovered

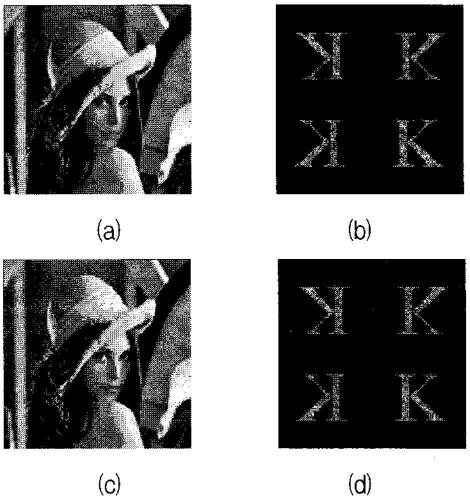


그림 12. 전송 영상 실수부의 JPEG 압축 시 전송 영상 및 복원 영상: (a) 75% JPEG압축 시 전송 영상, (b) 75% 압축 영상에 대한 복원 영상, (c) 50% JPEG압축 시 전송 영상, (d) 50% 압축 영상에 대한 복원 영상

Fig. 12. Transmitted and reconstructed image when JPEG compression is applied to the real part of the transmitted image: (a) 75% quality JPEG compressed transmitted image, (b) corresponding reconstructed image for 75% quality, (c) 50% quality JPEG compressed transmitted image, (d) corresponding reconstructed image for 50% quality

image is shown in Figs. 11(b), 11(d), and 11(f), respectively. Also, through the various simulations we can see that the location of the blocked pixels has no effect on the reconstructed image quality. Even with 75% blocking, the reconstructed image can be recovered. We also demonstrate the effect of applying JPEG compression on the transmitted image. The simulation is performed for JPEG compression of the transmitted image quality up to 75% and 50% from its original quality. Figure 12 shows the transmitted image and reconstructed image with JPEG compression. The values of the PSNR are 57.8 and 52.5 for the transmitted image quality of 75% and 50%, respectively.

## IV. Experiments

The validity of our proposed method was presented using the experimental setup for the optical

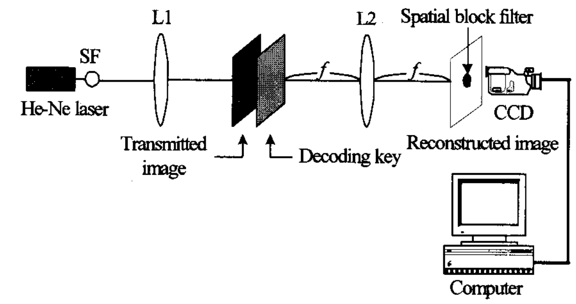


그림 13. 광학적인 복원 구조
Fig. 13. Optical reconstruction setup.

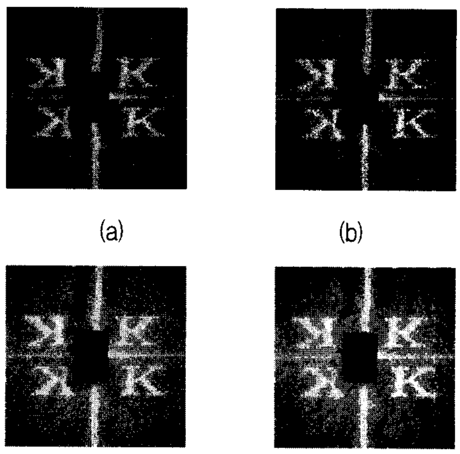

(a) (b)

(c) (d)

그림 14. 두 원 영상을 사용한 경우의 광 실험 결과: (a) 블록 되지 않은 전송 영상에 대한 복원 영상, (b) 25% 블록 된 전송 영상에 대한 전송 영상, (c) 50% 블록 된 전송 영상에 대한 전송 영상, (c) 75% 블록 된 전송 영상에 대한 전송 영상

Fig. 14. Results of optical experiment in case of the method with two original images: (a) reconstructed image with non-blocked transmitted image, (b) reconstructed image with 25% blocked image, (c) reconstructed image with 50% blocked image, (d) reconstructed image with 75% blocked image.

reconstruction system, as shown in Fig. 13. An Ar laser ($\lambda = 514$nm) beam is expanded by the spatial filter (SF) and is illuminated into the collimating lens (L1) and the transmitted image in the matching position by the decoding key. The transmitted image and the decoding key are placed on liquid crystal spatial light modulators (LC SLMs: HoloEye LC 2002 with pixel size 800×600) and the entire process is serially connected. Then the reconstructed image is on a CCD (PULNiX TM 1320-15CL with pixel size 1300×1030) plane through the Fourier lens (L2). The results of this experiment are shown in Figs. 14. We blocked the main lobe using a spatial block filter in the output plane. Figures 14(a),

14(b), 14(c), and 14(d) are the reconstructed image with non-blocked transmitted image, with 25% blocked transmitted image, with 50% blocked transmitted image, and with 75% blocked transmitted image, respectively, in case of the method with two images. Here, as we can see from the figure 14, even with 75% blocked, the reconstructed image can be recovered and the blocking of some pixels of the transmitted image has little affection the recovered image quality.

## V. Conclusion

It was proposed a novel watermarking method based on the multiple phase wrapping and real-valued decoding key to obtain a non-negative value for practical transmission. In order to improve the degree of security, the random patterns, used as the hidden image and the decoding key, are generated using the multiple phase wrapping.

This method has an advantage that the hidden data and the decoding key cannot be easily analyzed by illegal users due to nonlinear mapping in process of key generation. Hence, the degree of security for the proposed method is high owing to the use of the randomly distributed decoding key and the hidden image. Also, the information of the original image is not used in the reconstruction process. In addition, all the parameter used in embedding process is non-negative real value; this method is applicable to a variety of transmission systems practically. The process of reconstruction is very simple because of a serial connection setup that is advantageous in solving optical alignment and pixel-to-pixel mapping problems. By choosing suitable values of the coefficient of the invisibility and the visibility factor, background noise was reduced and the reconstructed image appeared outstanding. To demonstrate robustness to data loss of some pixels of the transmitted image, the PSNR properties of the reconstructed image were evaluated numerically when the transmitted image undergone cropping and JPEG compression. To confirm the validity of the proposed method, optical experiments also was performed. As a consequence of the simulation, it was confirmed that the proposed method was resilient to the distortion such as pixel cropping and JPEG compression.

## References


[1] A. Petitcolas, J. Anderson, and G. Kuhn, "*Information Hiding-A Survey,*" Proceeding of the IEEE, vol. 87, no. 7, July 1999.

[2] W. Bender, D. Gruhl, N. Morimoto, and A. Lu. "*Techniques for data hiding,*" IBM Systems Journal, vol. 35, no. 3 & 4, July 1996.

[3] W. Chen and C. Chen, "*Robust watermarking scheme for still images using frequently shift keying high-variance block selection,*" Optical Engineering, vol. 40, no. 11, Sep. 2001.

[4] Y. Aoki, "*Fresnel transform of images for application to watermarking,*" Electronics and Communications in Japan, Part 3, vol. 84, no. 12, 2001.

[5] N. Takai and Y. Mifune, "*Digital watermarking by a holographic technique,*" Applied Optics, vol. 41, no. 5, Nov. 2003.

[6] K. T. Kim, J. W. Kim, J. S. Lee, and J. U. Choi, "*Holographic Image Watermarking for Secure Content,*" Springer-Verlag Berlin Heidelberg 2004, LNCS 3184, 2004.

[7] D. Abookasis, O. Montal, O. Abamson, and J. Rosen, "*Watermarking encrypted in a concealogram and deciphered by a modified joint-transform correlator,*" Applied Optics, vol. 44, no. 15, May 2005.

[8] C. M. Shin, D. H. Seo, and S. J. Kim, "*Optical security system using multi-phase separation and phase-wrapping method,*" Journal of IEEK, vol. 42, no. 6, June 2005.

[9] S. Kishk and B. Javidi, "*Information hiding technique with double phase encoding,*" Applied Optics, vol. 41, no. 26, Sep. 2002.

[10] K. B. Cho, D. H. Seo, and S. J. Kim, "*Practical image hiding method using a multiple phase wrapping and real-valued decoding key,*" Optical Review, vol.14, no.3, May 2007.


## 저 자 소 개


조 규 보(정회원)
대한전자공학회 논문지
제 40권 SD편 3호 참조

이 승 희(정회원)
대한전자공학회 논문지
제 35권 D편 3호 참조

서 동 환(정회원)-교신저자
대한전자공학회 논문지
제 41권 SD편 6호 참조

홍 재 근(평생회원)
대한전자공학회 논문지
제 43권 TC편 10호 참조